

# Optimum service and seismic structural protection with adaptive dampers and base isolators for immediate occupancy after the earthquake

*P. Huber, M. Gruber*

MAURER SE, Munich, Germany.

*F. Weber*

Maurer Switzerland GmbH, Pfaffhausen, Switzerland.

## **ABSTRACT**

To improve serviceability of important civil structures during seismic action, base isolators and dampers need to perform with high efficiency independent of the ground shaking level. In service and seismic actions, base isolators/dampers should be able to adapt to the actual load cases. However, conventional devices are commonly designed to the shaking level of the Maximum Credible Earthquake (MCE) only, while their efficiencies are poor for lower peak ground accelerations (PGAs). This shortcoming can only be improved, if the friction and stiffness of curved surface sliders are not constant and if hysteretic dampers can produce hysteretic behaviour at different yield levels. This not only allows an optimum structural isolation system for the MCE with displacement control and acceleration limitation as conventional devices do, but moreover, it significantly improves structural service performance for weak and frequent earthquakes (DBE) with drastically reduced accelerations. This paper presents the functioning of two new types of devices: adaptive curved surface sliders and adaptive hysteretic dampers which operate at high efficiency over a wide range of PGAs. This enables significant enhancement of structural serviceability for weak/frequent earthquakes and ensures structural safety for the maximum earthquake. The dynamic behaviour of the new devices and the performance computed by non-linear time history analysis are presented. Enhanced isolation and damping performances are compared to conventional devices. With these new devices, immediate occupancy of structures even after severe earthquakes is possible. Structural and content damages can be almost completely avoided.

## 1 INTRODUCTION

Depending on the fundamental time period  $T_1$  of civil structures they are protected against seismic excitation either by base isolators ( $T_1$  in the plateau and first part of constant velocity range of response spectra) or inter-story hysteretic dampers ( $T_1$  in the second part of constant velocity range of response spectra). Base isolators such as Curved Surface Sliders (CSSs) decouple the structure from the shaking ground by their low coupling stiffness due to their large radius of curvature and add damping to the structure by friction damping. Due to the nonlinearity of friction damping CSS can be optimized to one shaking level, i.e., to one selected Peak Ground Acceleration (PGA) (Weber, et al. 2018), commonly the PGA of the Design Basis Earthquake (DBE). Hysteretic Dampers (HDs) produce a stiffness force when operated in their pre-yield region due to small inter-story relative motions while they exert a hysteretic damping force with low second branch stiffness when inter-story displacements are big enough to operate HDs in their post-yield region (Takeuchi, et al. 1999). That is why the behaviour of HDs can be described by a bilinear stiffness model or a hysteretic damper model as, e.g., the Bouc-Wen model.,

Because of the constant friction of conventional CSSs and the constant yield force of conventional HDs, the structural isolation by CSSs and the structural damping by HDs at low ground shaking levels due to weak but frequent earthquakes may be insufficient. This means that non-structural elements and sensitive equipment, which are crucial to ensure the serviceability of vulnerable structures such as hospitals, schools, government buildings, fire and police stations etc, are not efficiently protected. In order to overcome these drawbacks of conventional CSSs and HDs the following new adaptive types of CSSs and HDs are presented:

- Sliding Isolation Pendulum of type Adaptive: "SIP<sup>®</sup>-Adaptive"
- Modular Adaptive Shear Hysteretic Damper: "SHARK<sup>®</sup>-Adaptive"

Their dynamic behaviours are described by force displacement curves and the enhanced structural isolation is demonstrated by non-linear time history analysis.

## 2 SIP<sup>®</sup>-ADAPTIVE

### 2.1 Concept

The SIP<sup>®</sup>-Adaptive is a CSS with two primary sliding surfaces and an articulated slider that decouples the relative motions on both primary sliding surfaces (Figure 1, Figure 2). This basic feature allows designing the two primary sliding surfaces with different friction coefficients and different effective radii. The bottom sliding surface is designed with lower friction to active relative motion at low PGAs (below DBE). This primary sliding surface is constrained by a recess to limit its relative motion (Figure 2). Sliding surface 2 is designed with greater friction to provide the optimum damping at DBE and above. The effective radii are selected to produce the desirable softening behaviour at DBE to produce optimum structural isolation and increased stiffness and damping behaviours at the shaking level of the Maximum Considered Earthquake (MCE) to minimize the displacement demand of the SIP<sup>®</sup>-Adaptive.

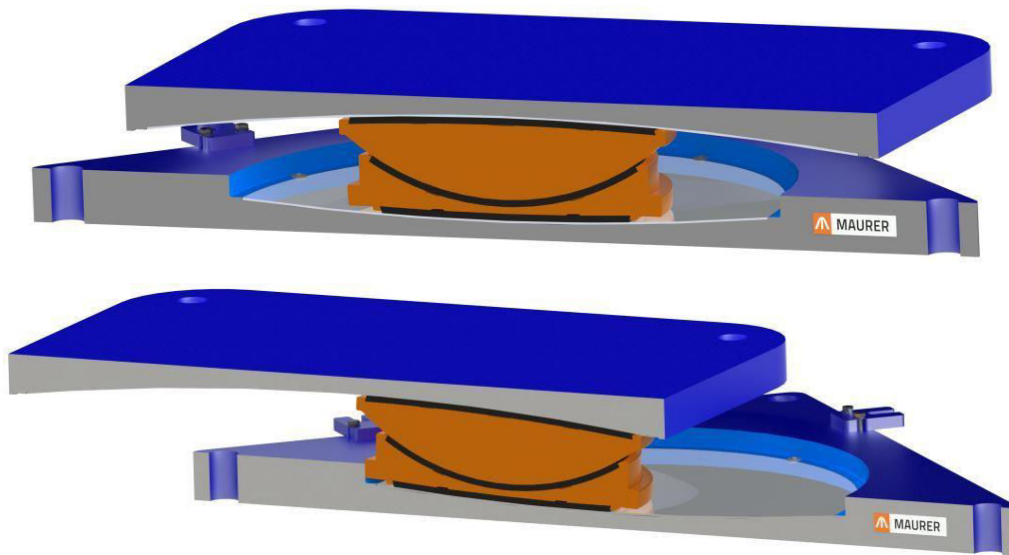


Figure 1: SIP<sup>®</sup>-Adaptive in centre position (above) and fully deflected position (below)

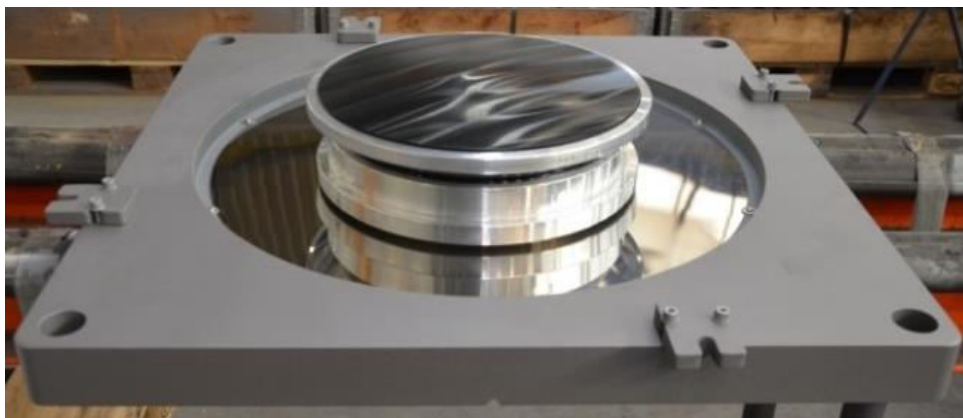


Figure 2: Bottom concave plate with recess and articulated slider of SIP<sup>®</sup>-Adaptive

## 2.2 Optimum design by dynamic simulation

The parameters of the SIP<sup>®</sup>-Adaptive, i.e., its friction coefficients, effective radii and displacement capacities of both primary sliding surfaces, are model-based optimized. For this the following model of the SIP<sup>®</sup>-Adaptive with superstructure is used (Figure 3). The superstructure with total mass  $m_s$  is modelled as linear and homogenous multi-degree-of-freedom (DOF) system with as many DOFs as storeys. The equations of motion of the upper bearing plate with mass  $m_2$  (including the fundament plate of the structure) and the slider mass with  $m_1$  become

$$m_2 \ddot{u}_2 + f_2 = c_s(\dot{u}_{s1} - \dot{u}_2) + k_s(u_{s1} - u_2) - m_2 \ddot{u}_g \quad (1)$$

$$m_1 \ddot{u}_1 + f_1 = f_2 - m_1 \ddot{u}_g \quad (2)$$

where the forces  $f_2$  and  $f_1$  describe the longitudinal forces on surfaces 2 and 1 that are given by the sum of the friction force given by the friction coefficients  $\mu_2$  and  $\mu_1$ , the restoring stiffness force due to the effective radii  $R_{eff-2}$  and  $R_{eff-1}$  and the linear stiffness force (recess stiffness  $k_{recess}$ ) of the recess of sliding surface 1 that is only activated at the displacement capacity  $d_1$

$$f_2 = \text{sgn}(\dot{u}_2 - \dot{u}_1) \mu_2 g (m_s + m_2) + (u_2 - u_1) \frac{g(m_s + m_2)}{R_{eff-2}} \quad (3)$$

$$f_1 = \text{sgn}(\dot{u}_1) \mu_1 g (m_s + m_2 + m_1) + u_1 \frac{g(m_s + m_2 + m_1)}{R_{eff-1}} + f_{recess} \quad (4)$$

$$f_{recess} = \begin{cases} 0 & : |u_1| \leq d_1 \\ k_{recess}(|u_1| - d_1) \text{sign}(u_1) & : |u_1| > d_1 \end{cases} \quad (5)$$

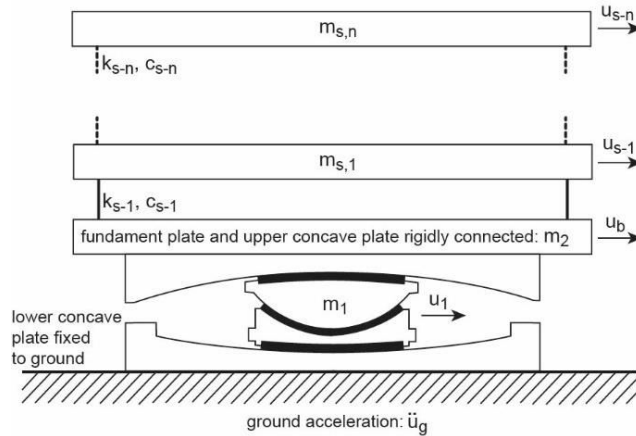


Figure 3: Sketch of structure (multi-DOF) with SIP<sup>®</sup>-Adaptive

The variables used in Equations (1-5) are:

- $\dot{u}_{s1}, u_{s1}$ : velocity, displacement of story 1 relative to ground
- $\ddot{u}_g$ : ground acceleration
- $\ddot{u}_2, \dot{u}_2, u_2$ : absolute acceleration, velocity and displacement relative to ground of the mass  $m_2$  (top bearing plate and fundament plate)
- $\ddot{u}_1, \dot{u}_1, u_1$ : absolute acceleration, velocity and displacement relative to ground of slider mass  $m_1$

The displacement capacity of sliding surface 2 is not constrained whereby the total displacement capacity of the SIP<sup>®</sup>-Adaptive is not limited as well. The coupled, stiff, and nonlinear differential equations (1-5) are

solved in the time domain using the Matlab<sup>®</sup>-solver ode15s(stiff/NDF) with maximum relative tolerance of 1e-3 and variable step size with upper bound of 1e-5 s.

### 2.3 Isolation performance

Absolute structural acceleration (~base shear) and total isolator displacement are computed by non-linear time history analysis for two different designs of the SIP<sup>®</sup>-Adaptive and compared to the conventional CSS with friction damping (CSS-FD) that is optimized at the PGA of the DBE (Figure 4, Figure 5). As theoretical benchmark the fully linear isolator with optimized linear viscous damping (CSS-VD) is computed as well. The following observations can be made:

- On the one hand, the SIP<sup>®</sup>-Adaptive reduces peak absolute structural acceleration within the entire PGA-range due to the fact that damping is smaller at lower shaking levels and damping is greater at higher shaking levels and, on the other hand, the total isolator displacement at MCE is smaller than for the CSS-FD due to the increasing stiffness and friction behaviours of the SIP<sup>®</sup>-Adaptive at shaking levels of the MCE.
- Due to the two friction values of the sliding surfaces 1 and 2 it is possible to tune the minimum base shear at lowest shaking levels by  $\mu_1$  (e.g. used as wind locking force) independently of the performance at DBE.

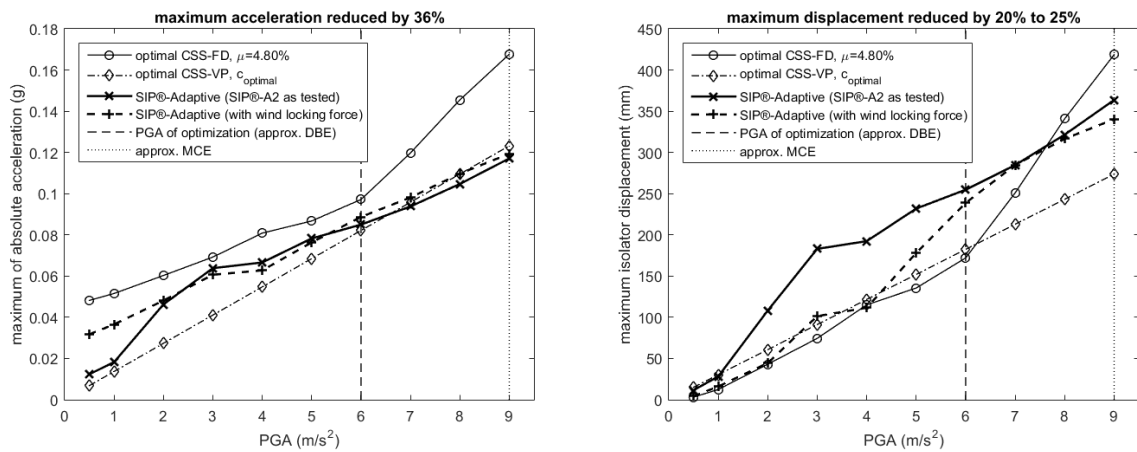


Figure 4: Computed absolute structural acceleration (left) and total displacement (right) of SIP<sup>®</sup>-Adaptive depending on ground shaking level

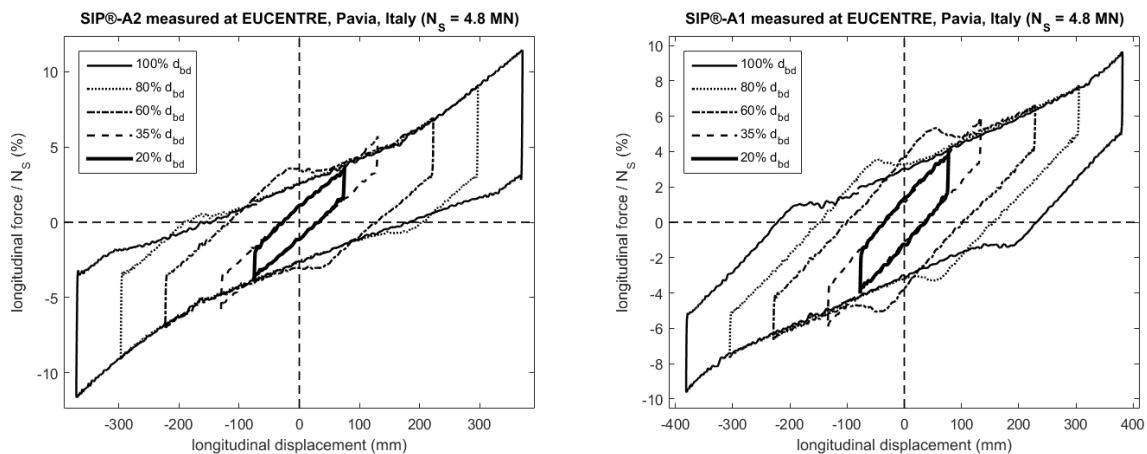


Figure 5: Measured (EUCENTRE, Pavia, left) force displacement characteristics of SIP<sup>®</sup>-A2 (left) and SIP<sup>®</sup>-A1

### 3 MODULAR SHEAR HYSTERETIC DAMPER SHARK<sup>®</sup>-ADAPTIVE

#### 3.1 Concept

Conventional shear hysteretic dampers (HD) are characterized by one yielding force which leads to the drawback of far suboptimal energy dissipation at low ground shaking levels because then the HD might not or only partially be operated in its yielding regime. Consequently, the damping provided to the structure is far below the maximum possible at PGAs significantly below the PGA of the DBE whereby the proper functioning of sensitive equipment of vulnerable buildings, e.g. hospitals, is not guaranteed. To overcome this problem and thereby enhance structural serviceability significantly the Modular Shear Hysteretic Damper SHARK<sup>®</sup>-Adaptive has been developed.

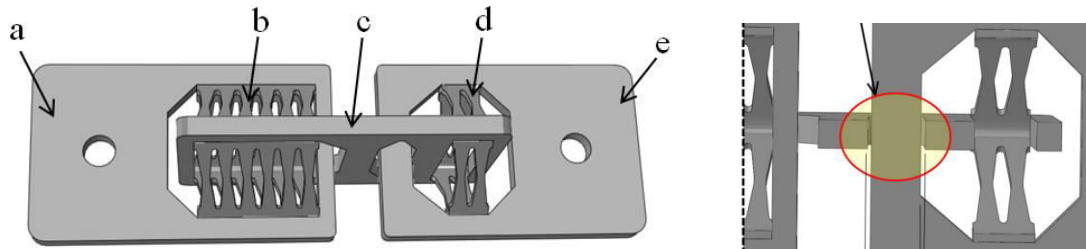


Figure 6: Sketch of entire SHARK<sup>®</sup>-Adaptive (left) and close-up of gap element of smaller hysteretic element (right)

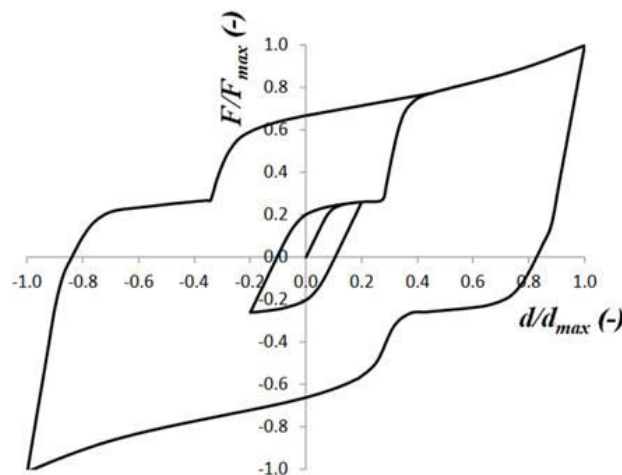


Figure 7: Force displacement curve of SHARK<sup>®</sup>-Adaptive computed by FEM

The basic working behaviour of this 2-stage hysteretic damper is as follows (a, e: main damper connecting plates):

- One smaller (d) and one bigger (b) shear hysteretic element are coupled in series by a connecting plate (c) with gap element (Figure 6).
- At low PGAs ( $\leq 50\%$  of DBE) the smaller hysteretic element is operated in its post-yield regime while yielding in the bigger element is not activated (Figure 7, small force displacement loop).
- At medium PGAs ( $\sim$ DBE) the smaller and the bigger hysteretic elements are activated (Figure 7, smaller and greater force displacement loops).
- At high PGAs ( $\sim$ MCE) the energy dissipation is dominated by the bigger hysteretic element which reduces maximum structural displacements.

## 3.2 Non-linear time history analysis of structure with SHARK<sup>®</sup>-Adaptive

### 3.2.1 Modelling

Non-linear time history analysis is performed for the 3-storey reinforced concrete building Hospital Lamezia Terme ( $T_1 = 0.7s$ ) that is located in a high-seismic area in southern Italy (Gandelli, et al. August 2019). The structure is modelled as linear shear frame and the common HD and the SHARK<sup>®</sup>-Adaptive, respectively, are modelled by the nonlinear hysteretic damper model. Seven site-specific accelerograms are used as ground excitation for each of the following ground shaking levels (according to Italian code):

- FDE (weak frequent earthquakes): 7 accelerograms with  $PGA = 0.17 \frac{m}{s^2}$
- DBE: 7 accelerograms with  $PGA = 0.45 \frac{m}{s^2}$
- MCE: 7 accelerograms with  $PGA = 0.50 \frac{m}{s^2}$

The dynamic simulations are performed in Matlab<sup>®</sup>/Simulink<sup>®</sup> adopting the same solver with same settings as used for the simulations of the SIP<sup>®</sup>-Adaptive.

### 3.2.2 HD design

The pushover analysis of the structure shows that plastic deformation in the columns occurs when the total deformation over all three stories is more than 0.45 % of entire structure height, i.e. 60 mm. The common HD is designed based on the approach (Gandelli, et al. August 2019) to avoid plastic deformation in the columns at DBE.

### 3.2.3 SHARK<sup>®</sup>-Adaptive design targets

The design of the SHARK<sup>®</sup>-Adaptive targets at achieving the following performances (Gandelli, et al. August 2019):

1. FDE: Reduced peak floor accelerations (PFA) to maximally protect sensitive equipment of the structure and ensure serviceability; inter-story drift  $\leq 0.5$  % to protect drift-sensitive non-structural elements (infills); this requirement is fulfilled here by the requirement on the total drift  $\leq 0.45$  %.
2. DBE: Ensure total structural deformation  $\leq 0.45$  % as for the HD.
3. MCE: Reduced maximum column deformations to increase structural safety at maximum ground shaking level.

### 3.2.4 Proposed SHARK<sup>®</sup>-Adaptive designs

The pre-yield and post-yield stiffness coefficients of the SHARK<sup>®</sup>-Adaptive are assumed to be equal to the values of the HD. The SHARK<sup>®</sup>-Adaptive design parameters are therefore:

- yielding force  $f_a$  of the smaller hysteretic element,
- size of gap element of the smaller hysteretic element, and
- yielding force  $f_b$  of the bigger hysteretic element.

Two solutions are derived by dynamic simulation fulfilling the design targets:

- SHARK<sup>®</sup>-Adaptive 1:  $f_{a-i} = 0.5 \cdot f_{HD-i}$ ,  $gap = [6.1; 5.8; 8.7]mm$ ,  $f_{b-i} = 1.32 \cdot f_{HD-i}$
- SHARK<sup>®</sup>-Adaptive 2:  $f_{a-i} = 0.6 \cdot f_{HD-i}$ ,  $gap = [5.9; 5.5; 8.5]mm$ ,  $f_{b-i} = 1.24 \cdot f_{HD-i}$

where  $f_{HD-i}$  denotes the yielding force of the common HD of storey  $i$ .

Table 1: Mean PFA and mean total structural displacement resulting from 7 FDE, DBE and MCE accelerograms

	ground shaking level	maximum displacement over all storeys [mm]	PFA storey 1 [g]	PFA storey 2 [g]	PFA storey 3 [g]
no HD	FDE*	far greater than 60	<b>0.257</b>	<b>0.295</b>	<b>0.374</b>
	DBE*	far greater than 60	0.731	0.933	1.390
	MCE*	far greater than 60	0.831	1.020	1.477
Common HD	FDE	21.4	<b>0.305</b>	<b>0.372</b>	<b>0.444</b>
	DBE	60	0.674	0.662	0.603
	MCE*	<b>75</b>	0.761	0.754	0.681
SHARK <sup>®</sup> -Adaptive -1	FDE	20.3	<b>0.249</b>	<b>0.288</b>	<b>0.257</b>
	DBE	60	0.782	0.666	0.711
	MCE*	<b>72</b>	0.787	0.720	0.766
SHARK <sup>®</sup> -Adaptive -2	FDE	21.8	<b>0.245</b>	<b>0.291</b>	<b>0.288</b>
	DBE	60	0.653	0.639	0.686
	MCE*	<b>71</b>	0.690	0.689	0.727

\*Computed with linear 3-dof model of structure

### 3.2.5 Results

The mean PFA and mean total structural displacement resulting from 7 accelerogram are given in Table 1 for the ground shaking levels FDE, DBE and MCE. The comparison of the data reveals:

- **Significantly reduced PFAs for weak earthquakes (FDE):** PFAs are reduced in average by 29.2 % by SHARK<sup>®</sup>-Adaptive-1 and 26.5 % by SHARK<sup>®</sup>-Adaptive-2.
- **Approximately same PFA at DBE:** If the design of the SHARK<sup>®</sup>-Adaptive aims at obtaining a reasonable PFA reduction at FDE (SHARK<sup>®</sup>-Adaptive-2 → -6.5 %) then the same average value of PFA at DBE can be achieved as for the HD. If the SHARK<sup>®</sup>-Adaptive design aims at further reducing PFAs (SHARK<sup>®</sup>-Adaptive-1 → -29.2 %) then the average PFA at DBE is marginal higher (+11.3 %).
- **Reduced total structural displacement at MCE:** The SHARK<sup>®</sup>-Adaptive reduces the maximum displacement over all storeys at MCE due to the bigger hysteretic element which enhances structural safety against unexpected too large plastic deformations.

### 3.3 Proof of concept

One shear hysteretic element of the SHARK<sup>®</sup>-Adaptive was tested at Bundeswehr University Munich (Figure 8). Besides the common force displacement measurements also strain measurements were made using a 3-dimensional scan optical system (Figure 9). The measurement data were used to further improve the FE-modelling to be able to extrapolate the FE-model for future design purposes (Figure 10).



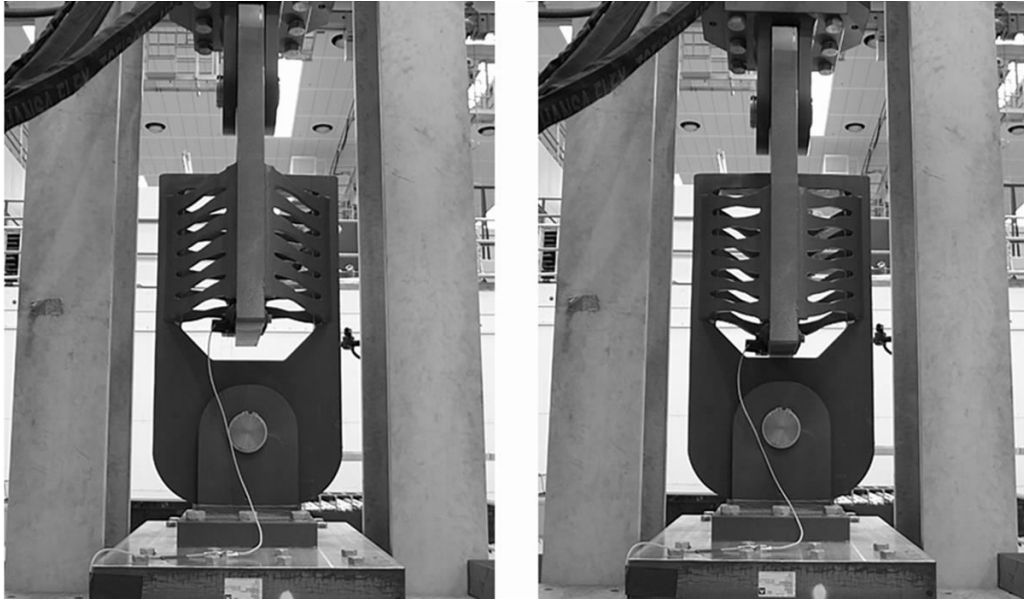


Figure 8: Testing one single hysteretic element of the SHARK®-Adaptive at Bundeswehr University Munich: left under max. elongation, right under max. compression

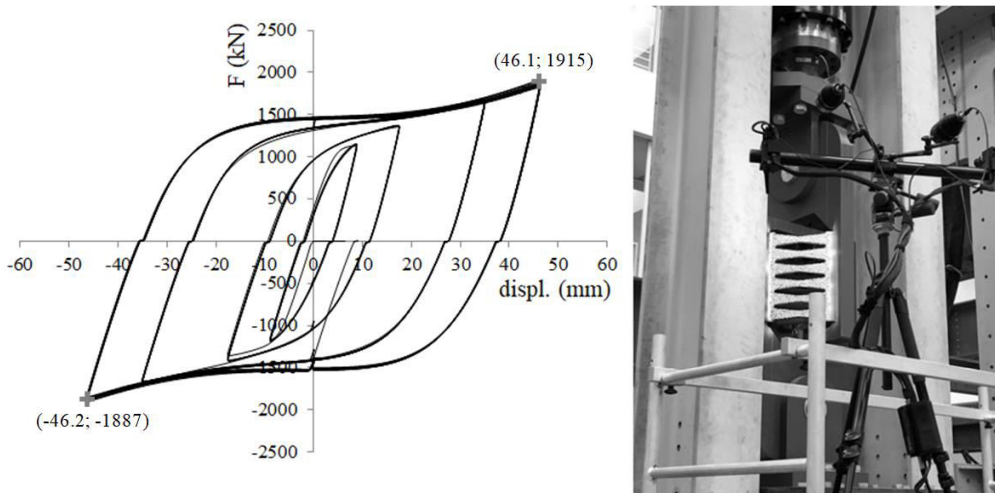


Figure 9: Measured force displacement curves (left) and 3-dimensional scan optical system (right)

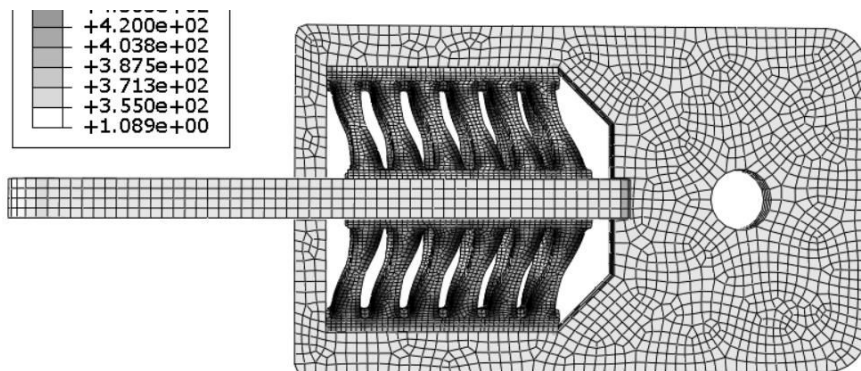


Figure 10: FE-modelling for stress analysis and optimization

## 4 CONCLUSIONS

The new base isolator SIP<sup>®</sup>-Adaptive and the new hysteretic damper SHARK<sup>®</sup>-Adaptive are presented. Both devices target at improving the seismic protection of structures and their sensitive equipment for frequent earthquakes with low to medium PGAs to enhance the serviceability of vulnerable structures such as hospitals, schools, government buildings, fire and police stations etc. The performance results of the SIP<sup>®</sup>-Adaptive demonstrate that this base isolator can reduce base shear within a large PGA range and – at the same time – the maximum isolator displacement at MCE. The results of the SHARK<sup>®</sup>-Adaptive point out that PFAs at weak and frequent earthquakes can be significantly reduced while guaranteeing approximately the same PFAs at DBE and reduced total structural displacements at MCE.

## 5 ACKNOWLEDGEMENTS

The authors gratefully acknowledge the support of all co-workers of the MAURER Group that contributed to these R&D projects.

## REFERENCES

- Gandelli, E, A Taras, J Distl, and V Quaglini. "Seismic Retrofit Of Hospitals By Means Of Hysteretic Braces: Influence On Acceleration-Sensitive Non-structural Components." *Frontiers in Built Environment*, August 2019: doi: 10.3389/fbuil.2019.00100.
- Takeuchi, T, H Nakamura, I Kimura, H Hasegawa, E Saeki, and A Watanabe. Buckling Restrained Braces And Damping Steel Structures. US Patent US20050055968A1. 1999.
- Weber, F, J Distl, L Meier, and C Braun. "Curved Surface Sliders With Friction Damping, Linear Viscous Damping, Bow Tie Friction Damping And Semi-Actively Controlled Properties." *Struct. Control Health Monitoring*, 2018: DOI: 10.1002/stc.2257.